The EMBO Journal Vol.17 No.7 pp.1883–1891, 1998

A distinct 14 residue site triggers coiled-coil formation in cortexillin I

Michel O.Steinmetz, Alexander Stock[1], Therese Schulthess[2], Ruth Landwehr[2], Ariel Lustig[2], Jan Faix[1], Günther Gerisch[1], Ueli Aebi[3] and Richard A.Kammerer[2]

M.E.Müller Institute for Microscopy and [2]Department of Biophysical Chemistry, Biozentrum, University of Basel, Klingelbergstrasse 70, CH-4056 Basel, Switzerland and [1]Max-Planck-Institut für Biochemie, D–82152 Martinsried, Germany

[3]Corresponding author
e-mail: aebi@ubaclu.unibas.ch

We have investigated the process of the assembly of the *Dictyostelium discoideum* cortexillin I oligomerization domain (Ir) into a tightly packed, two-stranded, parallel coiled-coil structure using a variety of recombinant polypeptide chain fragments. The structures of these Ir fragments were analyzed by circular dichroism spectroscopy, analytical ultracentrifugation and electron microscopy. Deletion mapping identified a distinct 14 residue site within the Ir coiled coil, Arg311–Asp324, which was absolutely necessary for dimer formation, indicating that heptad repeats alone are not sufficient for stable coiled-coil formation. Moreover, deletion of the six N-terminal heptad repeats of Ir led to the formation of a four- rather than a two-helix structure, suggesting that the full-length cortexillin I coiled-coil domain behaves as a cooperative folding unit. Most interestingly, a 16 residue peptide containing the distinct coiled-coil 'trigger' site Arg311–Asp324 yielded ~30% helix formation as monomer, in aqueous solution. pH titration and NaCl screening experiments revealed that the peptide's helicity depends strongly on pH and ionic strength, indicating that electrostatic interactions by charged side chains within the peptide are critical in stabilizing its monomer helix. Taken together, these findings demonstrate that Arg311–Asp324 behaves as an autonomous helical folding unit and that this distinct Ir segment controls the process of coiled-coil formation of cortexillin I.

Keywords: analytical ultracentrifugation/autonomous helical folding unit/circular dichroism spectroscopy/electron microscopy/heptad repeats

Introduction

Subunit oligomerization of many proteins is mediated by coiled-coil domains (Lupas, 1996; Kammerer, 1997; Kohn *et al.*, 1997). Typically, coiled coils consist of two to five right-handed amphipatic α-helices which coil around each other to form a slightly left-handed supercoil. Polypeptide segments giving rise to coiled coils are characterized by so-called heptad repeats of seven amino acid residues, denoted **a** to **g** (Sodek *et al.*, 1972; McLachlan and Stewart, 1975; Cohen and Parry, 1990). The residues at positions **a** and **d** are mostly apolar, thereby forming a 3,4-hydrophobic repeat with charged residues occurring frequently at the **e** and **g** positions. The hallmark of coiled coils is the distinctive packing of amino acid side chains in the hydrophobic core of the helix bundles, called 'knobs-into-holes' packing, which was first described by Crick (1953). Accordingly, hydrophobic interactions appear to represent the major driving force in stabilizing a coiled coil (Harbury *et al.*, 1993). Ionic interactions between the side chains of neighboring helices are considered relevant to the stability, orientation and stoichiometry of coiled coils (O'Shea *et al.*, 1992; Monera *et al.*, 1994; Zhou *et al.*, 1994; Beck *et al.*, 1997).

The simplicity and regularity of the coiled-coil structural motif have made it an attractive system for exploring some of the fundamental features of protein folding and protein–protein interactions. Moreover, coiled coils have been the focus of *de novo* protein design, a research area which has recently become important in attempts to rationally design multi-stranded coiled coils for a variety of purposes, including medical applications such as the targeting and delivery of drugs by heterodimerization technology, the engineering of synthetic biosensors and carrier molecules, and the discovery of new drugs (for a review see Hodges, 1996).

Although the parameters which determine the state of oligomerization and the stability of coiled coils are well known, only limited information is currently available on the mechanistic details leading to the formation of this apparently simple structural motif. Studies on the folding of coiled coils have primarily focused on tropomyosin, myosin and leucine zipper peptides, all producing two-helix structures. Thermodynamic and kinetic studies with leucine zippers suggested that their unfolding follows a simple two-state mechanism (Thompson *et al.*, 1993; Wendt *et al.*, 1995, 1997; Sosnick *et al.*, 1996). In contrast, the unfolding of the much longer coiled-coil domains of tropomyosin (Lehrer, 1978) and skeletal muscle myosin (King *et al.*, 1995) were reported to be non-two-state reactions indicating that these coiled coils may consist of discrete, independently stable subdomains. Kinetic studies using stopped-flow techniques with tropomyosin (Mo *et al.*, 1991, 1992), the leucine zipper domain of the yeast transcriptional activator GCN4 (a 33 residue peptide denoted GCN4-p1; Zitzewitz *et al.*, 1995; Sosnick *et al.*, 1996), and other leucine zipper peptides (Wendt *et al.*, 1995, 1997) suggested a fast bimolecular association step. However, none of these investigations established the mechanistic details underlying the folding pathway of coiled coils which in turn would not only be of theoretical but also, as mentioned above, of considerable practical value.

In this context, a rather puzzling, frequently made

observation is that relatively long heptad-repeat-containing polypeptide chain fragments derived from stable coiled-coil domains fail to associate into coiled-coil structures. For example, Trybus *et al.* (1997) have recently reported that smooth muscle myosin fragments with as many as 15 heptad repeats of the coiled-coil rod sequence failed to dimerize. This failure cannot be simply explained by instability due to the type of residues occupying the **a** and **d** positions of the heptad repeats, or by electrostatic repulsion of the two chains. As it is not known what factors determine chain association, the failure of chain assembly raises the question of whether there exist distinct sites within heptad-repeat-containing amino acid sequences which are necessary to mediate or initiate coiled-coil formation. We have addressed this question in detail by using the two-stranded coiled-coil oligomerization domain of cortexillin I (Ir), an actin cross-linking protein from *Dictyostelium discoideum* (Faix *et al.*, 1996). For this purpose, we produced a variety of fragments of Ir by heterologous gene expression in *Escherichia coli*, and investigated their structures and oligomeric states by circular dichroism (CD) spectroscopy, electron microscopy (EM) and analytical ultracentrifugation (AUC). Our data document that a distinct 14 residue segment exists within Ir that is absolutely required to mediate proper assembly of Ir into a parallel homodimeric coiled coil. Using a 16 residue synthetic peptide (cI-t), we further demonstrate that this coiled-coil 'trigger' site represents an autonomous helical folding unit. These novel findings suggest that coiled-coil formation is controlled by a helical trigger site(s).

Results

The oligomerization domain of cortexillin I forms a tightly packed, two-stranded, parallel coiled coil

Electron microscopic evidence, together with sequence analysis of cortexillin I predicting 18 continuous heptad repeats within its C-terminus, suggested that assembly of the parallel dimeric molecule is mediated by a coiled-coil oligomerization domain (Faix *et al.*, 1996). To test this hypothesis, we produced a recombinant polypeptide chain fragment corresponding to the predicted full-length oligomerization domain comprising residues 227–352 of *D.discoideum* cortexillin I in *E.coli* (Figure 1A and B). The homogeneity of the affinity-purified recombinant protein was assessed by tricine-SDS–PAGE (Figure 1C, lane 1) which revealed a single band consistent in size with the calculated molecular mass of the Ir monomer (15.0 kDa), with no obvious degradation products detected.

The oligomeric state of the recombinant Ir molecule was assessed by AUC. As shown in Table I, at 20°C in 5 mM sodium phosphate buffer (pH 7.4) containing 150 mM NaCl, the sedimentation equilibrium of Ir revealed an average molecular mass of 27.5 kDa, and sedimentation velocity yielded a sedimentation coefficient of 2.1S. These values are consistent with a dimeric rod-shaped conformation of Ir.

Inspection of the Ir molecules by transmission electron microscopy (TEM) after glycerol-spraying and rotary metal-shadowing yielded uniformly appearing, rod-shaped particles (Figure 2). The apparent length of the molecules was measured and put into a histogram (Figure 2, inset).

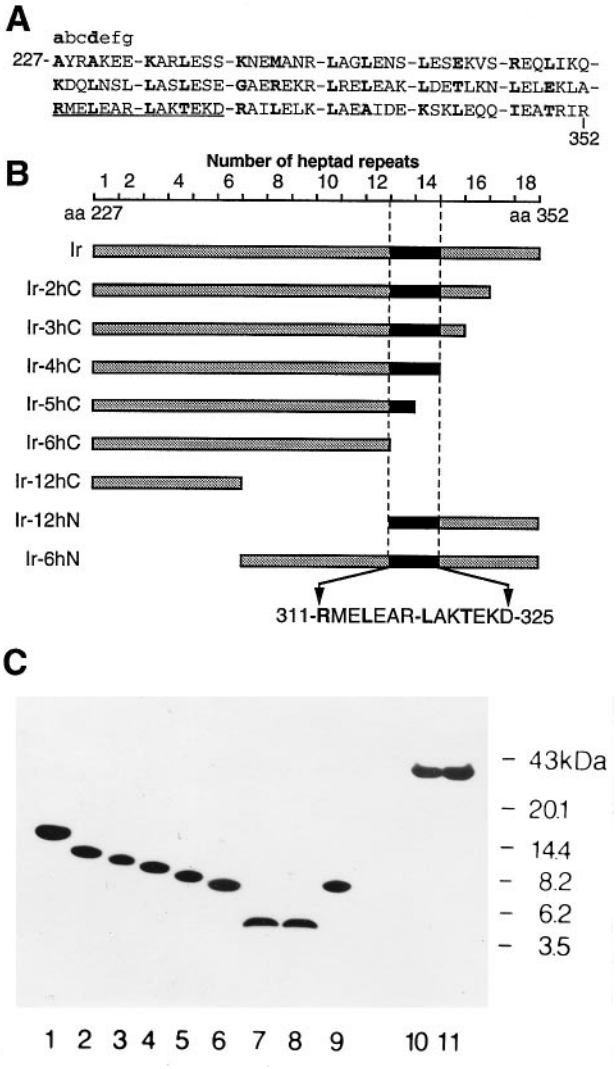

Fig. 1. Design and preparation of N- and C-terminal deletion constructs from Ir. (**A**) Amino acid sequence of Ir. Heptad repeats were assigned according to the COILS algorithm (Lupas *et al.*, 1991) and are shown in blocks of seven amino acid residues denoted abcdefg. Residues at heptad positions **a** and **d** are indicated in bold. The amino acid trigger site crucial for coiled-coil formation is underlined. (**B**) Schematic representation of Ir and various fragments thereof. The sizes of the polypeptide chain fragments are denoted on top by numbers of heptad repeats. The trigger site for coiled-coil formation is marked as a black box. (**C**) Tricine-SDS–PAGE of purified recombinant Ir fragments under reducing conditions. Lanes: 1, Ir; 2, Ir-2hC; 3, Ir-3hC; 4, Ir-4hC; 5, Ir-5hC; 6, Ir-6hC; 7, Ir-12hC; 8, Ir-12hN; 9, Ir-6hN; 10, cI-310; and 11, cI-324. The migration of marker proteins is given on the right in kDa.

A Gaussian fit of the histogram revealed a mean length of 19.2 ± 2 nm. This value is consistent with the mean length found for the tail domain of the native cortexillin I molecule (Faix *et al.*, 1996) as well as the calculated length of ~19 nm for a two-stranded, α-helical coiled-coil consisting of 18 continuous heptad repeats (with the assumption that the axial rise per residue corresponds to 1.485 Å; Fraser *et al.*, 1964).

Far-ultraviolet (UV) CD spectroscopy was employed to probe for the secondary structure of Ir. At 5°C and a total chain concentration of 35 μM, the CD spectrum recorded from Ir (Figure 3A) was characteristic for an α-helical coiled-coil structure exhibiting minima at 208 and 222 nm

Table I. Mean molar ellipticities at 222 nm, thermal melting temperatures at the midpoint of transition, sedimentation coefficients and molecular masses of the cortexillin I tail domain (Ir), and various Ir fragments and an Ir-derived peptide

Fragments	$[\Theta]_{222}$[a] (10^3 deg.cm^2/dmol)	T_m[b] (°C)	Sedimentation coefficient s_{20w}[c] (S)	molecular mass[d] (kDa)
Ir	–35.4	64	2.10	27.3 (15.0)
Ir-2hC	–30.9	55	1.58	24.7 (13.3)
Ir-3hC	–30.4	53	1.76	23.1 (12.6)
Ir-4hC	–27.5	51	1.60	22.9 (11.7)
Ir-5hC	–26.3	30	1.61	19.7/14.0[e] (10.9)
Ir-6hC	–21.2	n.d.	1.30	10.3 (10.1)
Ir-12hC	–5.7	n.d.	n.d.	4.9 (4.98)
Ir-12hN	–25.3	27	1.20	8.8 (5.24)
Ir-6hN	–36.7	63	2.17	39.7 (10.2)
cI-310	n.d.	n.d.	2.4	37.1 (35.4)
cI-324	n.d.	n.d.	2.9	71.0 (35.4)
cI-t	–9.2[f]	n.d.	n.d.	2.1[g] (1.92)

All fragments were analyzed in 5 mM sodium phosphate buffer (pH 7.4) containing 150 mM NaCl, except cI-t which was analyzed in 1 mM sodium phosphate buffer (pH 7.4). The corresponding amino acid sequences are shown schematically in Figure 1B.
[a]$[\Theta]_{222}$ measured at 5°C at chain concentrations (monomer) of 35 μM.
[b]T_m determined at chain concentrations (monomer) of 35 μM.
[c,d]Sedimentation coefficient and apparent molecular masses were determined at 20°C. The sequence-predicted monomer masses are enclosed in parentheses. Chain concentrations (monomer) varied from 0.1–0.5 mg/ml.
[e]Ir-5hC yielded a mixture of two predominant molecular species.
[f]Determined at 3°C at a peptide concentration of 30 μM.
[g]Determined at 3°C at two different peptide concentrations (300 and 30 μM) in the presence and absence of 100 mM NaCl.
n.d.: not determined

and a $[\Theta]_{222}$:$[\Theta]_{208}$ ratio of >1 (Zhou *et al.*, 1992). Based on a $[\Theta]_{222}$ value of –35 400 deg.cm^2/dmol (Table I), a helical content of >90% was estimated by assuming that a value of –37 300 deg.cm^2/dmol corresponds to a helicity of 100% for a 130 residue polypeptide chain fragment (Chen *et al.*, 1974). As expected for a non-covalently bonded, two-stranded α-helical coiled coil, the CD signal at 222 nm was concentration-dependent (data not shown).

The stability of the recombinant two-stranded α-helical coiled coil was assessed by thermal unfolding profiles recorded by CD at 222 nm. As shown in Figure 3B, at a total chain concentration of 35 μM, Ir revealed a single sharp melting profile characteristic for a cooperative helix–coil transition with a melting temperature (T_m) of 64°C. The thermal unfolding profile was monophasic and reversible with >95% of the starting signal being recovered upon cooling (data not shown).

To assess whether the hydrophobic core of the coiled coil was tightly packed, binding of the fluorescent dye 1-anilino-8-naphthalenesulfonate (ANS) to Ir was tested (Stryer, 1965; Jelesarov and Bosshard, 1996). Native proteins bind ANS weakly unless there is a solvent-accessible nonpolar region. At 20°C, addition of a 1- to 5-fold molar excess of ANS to a 35 μM Ir solution revealed an increase of the total fluorescence signal of <10% (data not shown) indicating no significant binding of the dye to the coiled coil.

To determine whether the helix orientation in the isolated two-stranded coiled-coil domain was parallel, as in the case of the native full-length cortexillin I molecule (Faix *et al.*, 1996), we recombinantly synthesized an Ir variant

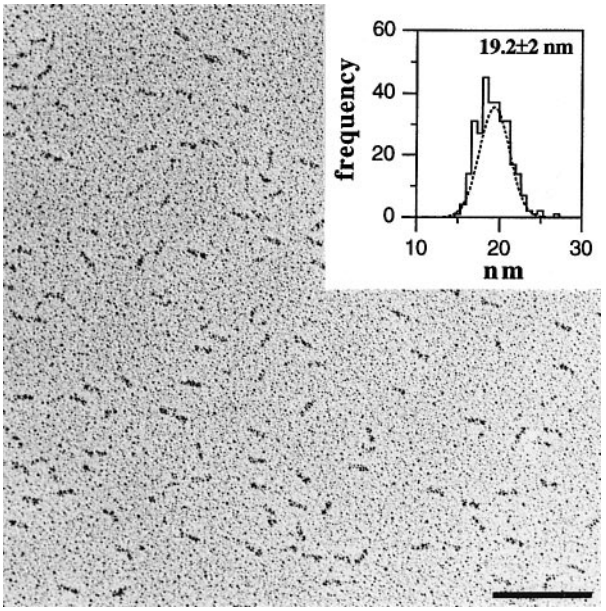

Fig. 2. Electron microscopic analysis of recombinant cortexillin Ir homodimer rods. Specimens were prepared by glycerol-spraying/rotary metal-shadowing. Scale bar, 100 nm. Inset, histogram with single Gaussian fit representing the distribution of the molecular length of Ir. One hundred and fifty molecules were measured, with the values displayed representing the mean and standard deviation of the histogram.

containing the GlyGlyCys sequence at its C-terminus. Non-reducing SDS–PAGE revealed a single ~30 kDa protein band, demonstrating that the two Ir chains assemble into a parallel dimer (data not shown).

Taken together, these results demonstrate that Ir associates into a tightly packed two-stranded, parallel, α-helical coiled coil which behaves as a single cooperative folding unit. This finding confirms the suggestion made by Faix *et al.* (1996) that the cortexillins represent a fourth class of molecules within the α-actinin/spectrin superfamily whose members are defined by a common F-actin binding motif, but are distinct from each other mainly in the design and architecture of their oligomerization domain (Matsudaira, 1991).

A distinct 14 residue site is necessary for coiled-coil formation of Ir

Ir was used as a model system to address the question of whether coiled-coil formation starts preferentially at a distinct site. Towards this goal, our strategy was to produce a number of Ir fragments and assess their ability to form coiled-coil structures by AUC and CD. First we produced, by heterologous gene expression in *E.coli*, four recombinant polypeptide chain fragments comprising the first six and twelve N-terminal (Ir-12hC and Ir-6hC, respectively) and the last six and twelve C-terminal (Ir-12hN and Ir-6hN, respectively) heptad repeats of Ir (Figure 1B and C). As the minimum length required for the formation of stable coiled coils has been reported to be in the range of 21–23 residues (Lumb *et al.*, 1994; Su *et al.*, 1994; Fairman *et al.*, 1995), these recombinant fragments were expected to be long enough to fold into stable coiled-coil structures. The homogeneity of the affinity-purified recombinant polypeptide chain fragments was assessed by tricine-SDS–PAGE, which revealed single bands with

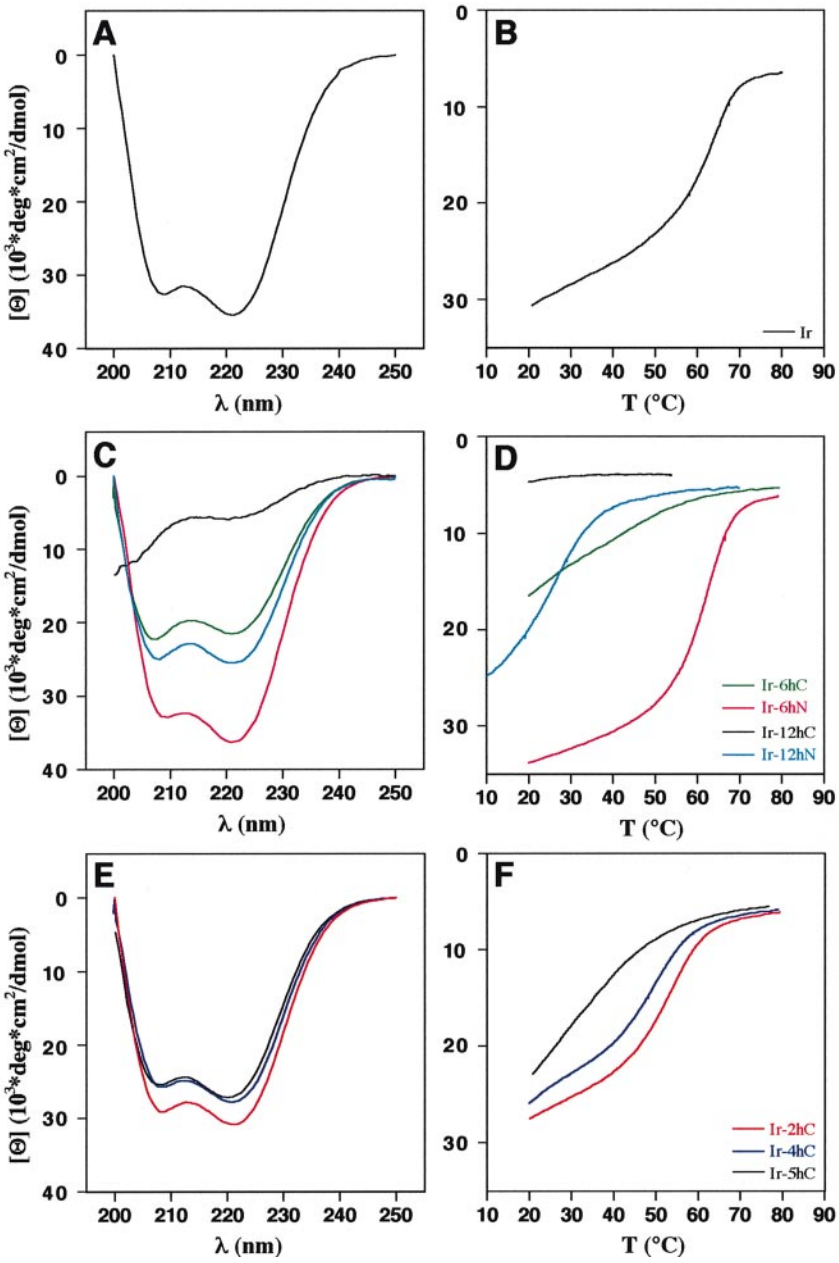

Fig. 3. CD measurements of recombinant cortexillin Ir and various deletion constructs. (A, C and E) Spectra recorded under native conditions at 5°C. (**A**) Ir. (**C**) Black curve, Ir-12hC; cyan curve, Ir-12hN; green curve, Ir-6hC; and magenta curve, Ir-6hN. (**E**) Red curve, Ir-2hC; blue curve, Ir-4hC; and black curve, Ir-5hC. For amino acid sequence, refer to Figure 1A and B. (**B**, **D** and **F**) Thermal unfolding profiles monitored by CD following the temperature-induced change of the mean molar residue ellipticity at 222 nm, $[\Theta]_{222}$. The same color code as for the spectra displayed in (A) and (C) was used. The total chain concentration was 35 μM for all seven fragments in 5 mM sodium phosphate buffer (pH 7.4) containing 150 mM NaCl.

mobilities corresponding to their calculated monomer molecular masses (Table I), with no degradation products detected (Figure 1C).

Deletion of six (Ir-6hC) or twelve (Ir-12hC) heptad repeats from the C-terminus of Ir completely abolished coiled-coil formation. AUC analysis of both Ir-6hC and Ir-12hC yielded average molecular masses of 10.3 and 4.9 kDa, respectively, which are consistent with the calculated monomer molecular masses (Table I). Surprisingly, Ir-6hC revealed a CD spectrum indicating a substantial amount of helicity at 5°C (Figure 3C, green curve). However, its CD spectrum was characteristic for partial monomer helix formation as evidenced by its insignificant concentration dependence (data not shown), a shift of the minimum from 208 to 205 nm and a $[\Theta]_{222}$:$[\Theta]_{205}$ ratio of <1. Moreover, its corresponding thermal unfolding profile exhibited a very broad, non-cooperative transition (Figure 3D, green curve). Finally, glycerol-sprayed/rotary metal-shadowed Ir-6hC molecule samples produced specimens which appeared rather heterogeneous in the EM in terms of particle size and shape (data not shown). Ir-12hC, on the other hand, revealed a CD spectrum at 5°C typical for proteins in a random coil conformation with a pronounced minimum at 200 nm (Figure 3C, black curve). As expected, this Ir fragment yielded no significant thermal unfolding profile (Figure 3D, black curve).

In contrast, deletion of six (Ir-6hN) or twelve (Ir-12hN) heptad repeats from the N-terminal end of Ir did not significantly affect coiled-coil formation (Figure 3C and D, magenta and cyan curves; Table I). Both fragments yielded concentration-dependent CD spectra characteristic for α-helical coiled-coil structures (Figure 3C), and the corresponding thermal unfolding profiles at a chain concentration of 35 μM exhibited cooperative transitions with T_ms of 63 and 27°C for Ir-6hN and Ir-12hN, respectively (Figure 3D; Table I). Rather surprisingly, sedimentation equilibrium revealed that the Ir-6hN fragment forms a tetramer (Table I). Electron micrographs of glycerol-sprayed/rotary metal-shadowed Ir-6hN yielded uniformly distributed, elongated particles which appeared shorter but somewhat thicker than corresponding Ir particles (data not shown). An average molecular length of 12.8 ± 1.2 nm was determined for Ir-6hN, which is exactly two-thirds of the full-length Ir molecule. Together with the data obtained by CD, these findings suggest a four-stranded, most likely unstaggered coiled-coil structure of Ir-6hN.

Based on these findings, we next focused our attention on the last six C-terminal heptad repeats (Arg311–Arg352) of Ir. To map more precisely the critical site for coiled-coil formation, we prepared chain variants missing two (Ir-2hC), three (Ir-3hC), four (Ir-4hC) or five (Ir-5hC) heptad repeats from the C-terminus of Ir (Figure 1B and C). Deletions of up to four heptad repeats from the C-terminus of Ir retained the ability of the corresponding Ir fragments for coiled-coil formation (Figure 3E and F; Table I). Ir-2hC (red curve), Ir-3hC (data not shown) and Ir-4hC (blue curve) all had features reminiscent of two-stranded coiled-coil structures as revealed by their α-helical CD spectra (all concentration-dependent; data not shown), cooperative thermal unfolding profiles (T_m values of 55, 53 and 51°C, respectively, at a chain concentration of 35 μM; Table I), and AUC sedimentation velocity profiles and sedimentation equilibrium boundaries characteristic for elongated dimeric molecules (Table I). In contrast, whereas Ir-5hC (Figure 3E and F, black curve) still yielded a mixture of monomers and dimers, deletion of more than five heptad repeats from the C-terminus of Ir resulted in the complete loss of homodimer formation as revealed by AUC (see above and Table I).

Taken together, deletion mapping identified a distinct 14 residue site, Arg311–Asp324, which was absolutely necessary to trigger the assembly of the oligomerization domain of cortexillin I into a two-stranded, parallel, α-helical coiled coil. To confirm our findings further, we prepared two cortexillin I fragments, cI-310 and cI-324, which were designed so as to contain the N-terminal globular head domain (residues 1–226) together with 12 (cI-310) or 14 (cI-324) heptad repeats of its coiled-coil domain. Remarkably, electron micrographs of glycerol-sprayed/rotary metal-shadowed cI-310 molecules which were missing the critical sequence Arg311–Asp324 yielded uniformly distributed, apparently monomeric globular particles (Figure 4A). The 4–6 nm diameter particles evidently represented the N-terminal actin-binding domain (residues 1–226 of cortexillin I; Faix *et al.*, 1996). In contrast, cI-324, which differs from cI-310 only in the critical 14 residues Arg311–Asp324 revealed dimeric molecules consisting of two globular heads attached to one end of a ~15 nm long stalk (Figure 4B). With the exception of a ~4 nm shorter rod, the overall morphology of the dimeric cI-324 particles appeared very similar to that of glycerol-sprayed/rotary metal-shadowed native cortexillin I (Faix *et al.*, 1996). These EM-based findings were confirmed by AUC measurements yielding average molecular masses of 37.1 kDa (calculated monomer mass 35.4 kDa) for cI-310 and 71.0 kDa (calculated monomer mass 37.1 kDa) for cI-324 (Table I).

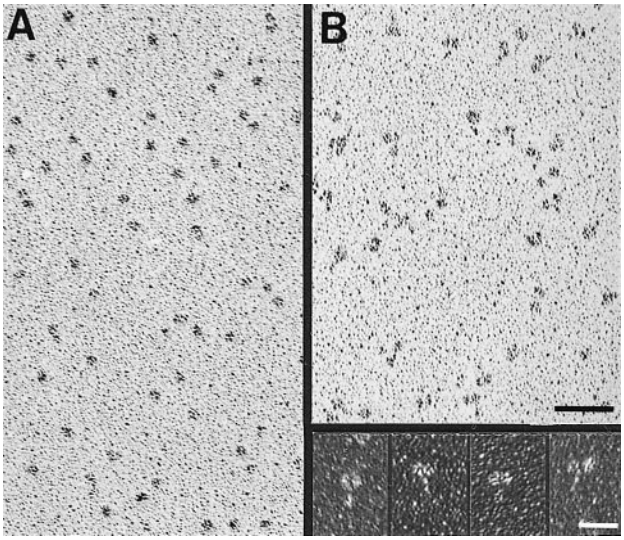

Fig. 4. Electron micrographs of glycerol-sprayed/rotary metal-shadowed recombinant (**A**) cI-310 and (**B**) cI-324 cortexillin I fragments which were designed so as to contain the N-terminal globular head domain (residues 1–226) and 12 or 14 heptad repeats, respectively, of the coiled-coil oligomerization domain, Ir. Scale bars, 50 nm for low magnification overviews and 25 nm for high magnification gallery.

The coiled-coil 'trigger' site represents an autonomous helical folding unit

To characterize the coiled-coil trigger site further, we synthesized the 16 residue peptide Ac-ARMELEARLAK-TEKDR-NH_2 (Ala310–Arg325), denoted cI-t, and analyzed its structure and oligomeric state by CD and AUC. As illustrated in Figure 5A, at 3°C and in 1 mM sodium phosphate, pH 7.4, the far-UV CD spectrum of cI-t was characteristic for partial helix formation with well-defined minima at 222 nm (α-helix n–π* transition) and 203 nm (mixture of α-helix π–$\pi_{\|}$* transition and random coil π–π* transition). Helix formation by the peptide was monomolecular as shown by AUC (Table I) and the lack of any significant concentration dependence of $[\Theta]_{222}$ in the range of 20–200 μM (data not shown). Based on the $[\Theta]_{222}$ value of –9200 deg.cm^2/dmol, a helical content of ~30% was estimated by assuming that a value of –30 000 deg.cm^2/dmol corresponds to 100% helicity for a 16 residue peptide (Chen *et al.*, 1974).The monomeric helix formed by cI-t unfolds rapidly with increasing temperature as evidenced by a shift in wavelength of the minimum from 203 to 200 nm at higher temperatures and a concomitant decrease of $-[\Theta]_{222}$ (Figure 5A).

The helix content of cI-t has also been measured as a function of pH and ionic strength. The helix content of cI-t at 3°C was strongly pH-dependent: $-[\Theta]_{222}$ decreased moderately as the pH was raised above 2 and decreased significantly as the pH was increased above 11 (Figure 5B,

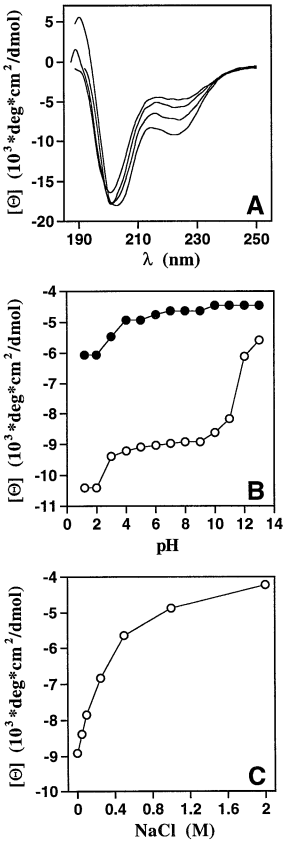

Fig. 5. CD analysis of the 16 residue peptide cI-t. (**A**) Far-UV CD spectra at 3, 10, 20 and 50°C in 1 mM sodium phosphate buffer, pH 7.4. The increasing temperature led to a shift in the wavelength of the minimum from 203 to 200 nm and a concomitant decrease of $-[\Theta]_{222}$. (**B**) pH dependence of $[\Theta]_{222}$ at 3°C (open symbols) and at 50°C (filled symbols) in 1 mM sodium citrate, 1 mM sodium phosphate and 1 mM sodium borate buffer. (**C**) NaCl dependence of $[\Theta]_{222}$ at 3°C in 1 mM sodium phosphate buffer, pH 7.4. The peptide concentration was 30 μM for all experiments.

open symbols). This pH effect was drastically attenuated at 50°C where the helix was largely melted (Figure 5B, filled symbols). A strong decrease in the helix content of cI-t was also observed upon raising the ionic strength from 0 to 2 M NaCl (Figure 5C). Throughout the pH range and salt concentrations evaluated, helix formation remained temperature-dependent and occurred in a monomolecular reaction. These results suggest that electrostatic interactions of charged amino acid side chains are critical in stabilizing the cI-t monomer helix.

Discussion

A coiled-coil trigger site is absolutely necessary for chain assembly of cortexillin I

The two-stranded parallel coiled coil is the simplest representative of multi-subunit proteins with only one type of secondary- and a well-defined quartenary-structure. This structural motif has been used extensively as a model system for studying both the intra- and intermolecular interactions which govern the folding and stability of multimeric proteins. As a consequence of (i) thermodynamic studies of naturally occurring coiled-coil proteins (Lehrer, 1978; O'Shea *et al.*, 1989), (ii) the design and characterization of simple peptides of diverse length and sequence (for a review see Betz *et al.*, 1995), and (iii) determination of the crystal structure of a number of coiled-coil proteins (Malashkevich *et al.*, 1996; for review see Lupas, 1996; Kohn *et al.*, 1997), the interactions which stabilize coiled coils and specify their oligomerization state are now fairly well understood. Information on the mechanistic details of the coiled-coil assembly process, however, has remained rather limited. For example, the observation that fragments of considerable length derived from stable coiled-coil domains failed to oligomerize (Trybus *et al.*, 1997) has been difficult to explain.

For this reason, we have addressed the question of whether there exist distinct sites within coiled coils which are necessary to mediate chain assembly of heptad-repeat-containing segments. We have chosen the coiled-coil oligomerization domain of *D.discoideum* Ir as a model polypeptide for the following three reasons (for details see Results). (i) Ir forms a tightly packed parallel homodimer which represents the simplest type of coiled-coil structure. (ii) The full-length Ir domain is of intermediate size and is exceptional in the sense that it consists of 18 continuous heptad repeats which are not interrupted by any discontinuities such as stutters, stammers or skip residues (Brown *et al.*, 1996). Generally, in two-stranded coiled coils the average length of a continuous heptad-repeat segment is only ~80 residues (i.e. 11–12 heptad repeats; Conway and Parry, 1991). As the minimum length required for the formation of stable coiled coils has been reported to be in the range of 21–23 residues (Lumb *et al.*, 1994; Su *et al.*, 1994; Fairman *et al.*, 1995), our recombinant Ir fragments (Figure 1B) were expected to be long enough to fold into stable coiled-coil structures. (iii) Ir exhibits cooperative, two-state unfolding and refolding, which suggests that the dimer represents a uniform and entire folding domain.

Using a systematic N- and C-terminal deletion mapping strategy (Figure 1) we have identified a 14 residue segment, Arg311–Asp324, which was absolutely required for triggering oligomerization of cortexillin I. Deletion of this specific coiled-coil trigger site completely abolished dimerization of up to 12 heptad repeat long Ir fragments. This finding may explain why in some cases the presence of heptad repeats is not sufficient to mediate stable coiled-coil formation (Trybus *et al.*, 1997). Finally, the observation that Ir-4hC and Ir-12hN formed stable coiled-coil structures indicates that folding can occur from the trigger site in both the N- and C-terminal directions.

Deletion of N-terminal heptad repeats alters the state of oligomerization of Ir

Deletion of the first six N-terminal heptad repeats of Ir (Ir-6hN) yielded tetramers, as revealed by AUC. Moreover, CD thermal unfolding profiles exhibited a monophasic cooperative transition, and AUC measurements at varying ionic strength (data not shown) suggested a four-stranded coiled-coil structure for Ir-6hN rather than a tetramer formed by the association of two two-stranded coiled coils. In agreement with this suggestion, inspection of metal-shadowed Ir-6hN specimens by TEM revealed rod-shaped particles whose length was consistent with the calculated length of ~13 nm for an unstaggered four-stranded coiled coil consisting of four 86 residue chains.

The formation of different oligomerization states of

coiled coils was explained in terms of packing geometries of the **a** and **d** position amino acid side chains in the hydrophobic core (Harbury *et al.*, 1993, 1994). However, it has recently been documented that the **e** and **g** positions flanking the **a** and **d** sites can significantly influence the oligomerization specificity of coiled coils. For example, by replacing a single amino acid residue at the heptad positions **e** (Kammerer *et al.*, 1998) or **g** (Beck *et al.*, 1997) within the coiled-coil domains of tenascin-C and matrillin I, these authors observed a switch from three- to four-stranded coiled-coil structures. The hydrophobic interface of four-stranded coiled coils is more extended relative to that of dimers and trimers (Harbury *et al.*, 1993, 1994): the **e** and **g** sites in the tetramer are almost as deeply buried as the **a** and **d** positions in the dimer (Harbury *et al.*, 1993). As hydrophobic packing is the major driving force of coiled-coil formation, removal of particular heptad repeats or even substitution of single amino acid residues may allow for a more favorable packing of the **e** and **g** residues in the tetramer conformation. Moreover, the tetramer also exhibits several types of interchain ionic interactions that are not observed in the dimer (**g** to **b**′ and **c** to **e**′, i.e. between residue i in one chain and residue i′+2 in the neighboring chain; Harbury *et al.*, 1993, 1994).

Taken together, these findings suggest that the full-length cortexillin I coiled-coil domain behaves as a cooperative folding unit and that its oligomerization state is specified by the arrangement and number of heptad repeats. Deletion of particular heptad repeat segments distinct from the coiled-coil trigger site alters this context, and therefore may result in a switch of the oligomerization state.

The coiled-coil trigger site of cortexillin I represents an autonomous helical folding unit

Most interestingly, we found that the 16 residue cI-t peptide which contains the coiled-coil trigger site (Arg311–Asp324) of Ir folded into a monomeric helix exhibiting 30% helicity at 3°C and pH 7.4. Generally such short peptides are not stable in aqueous solution unless they contain a special sequence (for review see Scholtz and Baldwin, 1992; Dyson and Wright, 1993). Analysis of the primary amino acid sequence of cI-t revealed that 11 out of 16 residues occur with high frequencies in α-helices (A, R, K, L and M). These residues are known to exhibit the strongest helical propensities among all naturally occurring amino acids (Parthasarathy *et al.*, 1995). Furthermore, helix formation by cI-t was strongly dependent on pH and ionic strength. Variation of these parameters revealed differences in helicity of up to a factor of two, demonstrating that electrostatic interactions (e.g. charge–helix dipole interactions or electrostatic side-chain–side-chain interactions) are critical for stabilizing the cI-t monomer helix. Three favorable, putative helix-stabilizing, i, i+4 intrachain ionic interactions (Marqusee and Baldwin, 1987) can be assigned to cI-t, for example. As other 14 residue sites with three or even four positive i, i+4 attractive ion pairs exist within Ir, the coiled-coil trigger sequence is not different from other two-heptad repeat segments in terms of intrahelical electrostatic interactions. Although the peptide's pH titration curve is difficult to interpret due to the presence of several charged residues, a rough estimation suggests that protonation of lysine residues (pK_a = 10.8) is the main cause of the pH-dependent helix-stabilizing effect in cI-t (Figure 5B). Taken together, these findings are consistent with cI-t representing an autonomous helical folding unit (Shoemaker *et al.*, 1987; Scholtz and Baldwin, 1992).

Towards dissecting the mechanistic details of coiled-coil formation

For productive oligomer formation of coiled coils to occur, it is reasonable to assume that some partial folding of the monomer species may be required. Recent measurements of the kinetics of helix unfolding, both in a peptide (Williams *et al.*, 1996) and in a protein (Gilmanshin *et al.*, 1997), have indicated that helix unfolding and refolding occur on a time scale of 10^{-7} s or faster. Because helix nucleation is ten times faster than the fastest loop closure reaction (Eaton *et al.*, 1997), it follows that incipient helices are already present when formation of the tertiary structure begins. As the monomeric peptide cI-t revealed significant helicity in aqueous solution, we may speculate that the process of chain assembly in native cortexillin I is controlled by helix formation at the coiled-coil trigger site Arg311–Asp324. One feature of the trigger site which might be important in this context is the presence of a putative interhelical, **g** to **e**′, attractive ionic interaction between Arg317 of one chain and Glu322 of the other (i.e. between residue i and residue i′+5; O'Shea *et al.*, 1991). This interaction may be important in the chain–chain recognition and in-register alignment process at some stage in the folding pathway. From the interacting trigger sites, helices then propagate along the molecule to form finally a stable two-stranded coiled coil. Clearly, the heptad repeats involved in the elongation process are important for the overall stability and stoichiometry of the final structure. Such a mechanism might explain the fast folding rates observed for two-stranded coiled coils of varying length (Mo *et al.*, 1991, 1992; Wendt *et al.*, 1995; Zitzewitz *et al.*, 1995; 1997; Sosnick *et al.*, 1996). It should be noted, however, that the ability of a chain segment to fold into a stable monomer helix is probably not sufficient to mediate proper coiled-coil formation. The CD spectrum of Ir-6hC, for example, was characteristic for 50–60% helix formation. However, the fragment was clearly monomeric, as revealed by AUC and by its concentration-independent CD signal at 222 nm. Moreover, Ir-6hC exhibited a broad non-cooperative thermal unfolding CD profile. The possibility that Ir-6hC forms an antiparallel coiled coil in which the monomeric chain folds back on itself therefore cannot be completely ruled out.

Coiled-coil regions of different stabilities, in turn, may be important for regulatory or mechanical processes as has recently been proposed by Tripet *et al.* (1997). Interestingly, these authors found that conserved 'non-ideal' residues located within hydrophobic positions of the two central heptad repeats of the kinesin neck destabilize the two-stranded, parallel coiled coil. Based on this finding, Tripet *et al.* (1997) concluded that these non-ideal residues may enable a portion of the coiled coil to unwind cooperatively during kinesin motility.

Clearly, kinetic folding and unfolding measurements of wild-type and mutant Ir molecules and fragments thereof

will now be necessary to elucidate more rigorously the exact role of the coiled-coil trigger site.

Materials and methods

Construction of expression plasmids

cDNA of full-length *D.discoideum* cortexillin I (Faix *et al.*, 1996) was used as a template for PCR amplification of DNA fragments encoding residues 227–352 (Ir), 227–338 (Ir-2hC), 227–331 (Ir-3hC), 227–324 (Ir-4hC), 227–317 (Ir-5hC), 227–310 (Ir-6hC), 227–268 (Ir-12hC), 311–352 (Ir-12hN), 269–352 (Ir-6hN), 1–310 (cI–310) and 1–324 (cI–324). For Ir, oligonucleotides were designed to obtain a *Nde*I site at the 5′ end (CCTCCCATATGGCCTATAGAGCCAAGGAAGAG) and two translation stop signals TAA followed by a *Bam*HI site at the 3′ end (CCCGGATCCTTATTATCTGATTCTGGTGGCTTCGAT). For the Ir fragments, primers were designed to obtain either a *Nde*I (Ir-2hC, Ir-3hC, Ir-4hC and Ir-5hC: same 5′ primer as for Ir) or a *Bam*HI site at the 5′ end (Ir-6hC and Ir-12hC, CCCGGATCCGCCTATAGAGCCAAGGAAGAG; Ir-12hN, CCCGGATCCCGTATGGAACTCGAAGCAAG; and Ir-6hN, CCCGGATCCAAGGATCAACTCAATAGTTTATTG) and two TAA stop codons preceding a *Bam*HI site (Ir-2hC, CCCGGATCCTTATTATTCATCGATGGCTTCAGCTAAT; Ir-3hC, CCCGGATCCTTATTATTTCAATTCCAAGATAGCTCTATC; Ir-4hC, CCCGGATCCTTATTAATCCTTTTCGGTCTTGGCTAAT; Ir-5hC, CCCGGATCCTTATTATCTTGCTTCGAGTTCCATACG; Ir-6hC, CCCGGATCCTTATTAAGCCAATTTCTCTAATTCCAA; Ir-12hC, CCCGGATCCTTATTATTGTTTGATTAATTGTTCACGTG; Ir-12hN and Ir-6hN, same 3′ primer as for Ir) at the 3′ end. Four cI-310 and cI-324 primers were designed to obtain a *Bam*HI site preceding an FXa cleavage site at the 5′ end (CGCGGATCCCAATCGAAGGTCGTATGGCAGGTAAAGATTGGGAAATA) and a TAA stop codon followed by a *Hin*dIII site (cI-310, CCCAAGCTTTTAAGCCAATTTCTCTAATTCCAA; cI-324, CCCAAGCTTTTAATCCTTTTCGGTCTTGGCTAA) at the 3′ end.

The amplified products were ligated into the following bacterial expression vectors: pET–15b (Novagen) at *Nde*I–*Bam*HI sites (Ir, Ir-2hC, Ir-3hC, Ir-4hC and Ir-5hC); pPEP–T (Brandenberger *et al.*, 1996) at *Bam*HI–*Bam*HI sites (Ir-6hC, Ir-12hC, Ir-12hN and Ir-6hN); and pQE–32 (Qiagen) at *Bam*HI–*Hin*dIII restriction sites (cI-310 and cI-324). The inserted sequences of all constructs were verified by Sanger dideoxy DNA sequencing.

Production and purification of recombinant cortexillin I fragments

The *E.coli* host strains JM109(DE3) (Promega) for pPEP–T and pET–15b and M13 (Qiagen) for pQE–32-expression plasmids were used for expression. Production and affinity purification of His_6-tagged fusion proteins by immobilized metal affinity chromatography (IMAC) on Ni^{2+}-Sepharose (Novagen) was performed under denaturing (all Ir fragments) or non-denaturing (cI-310 and cI-324) conditions as described in the manufacturer's instructions. Separation of recombinant fragments from the His_6-tag or from the His_6-tagged carrier protein by thrombin cleavage was carried out as described by Kammerer *et al.* (1995). FXa (Boehringer Mannheim) cleavage was performed at 10°C for 72 h in 50 mM Tris, pH 8.0, 100 mM NaCl, 2 mM $CaCl_2$ at an enzyme:substrate stoichiometry of 1:2000. Polypeptide chain fragments obtained from pPEP–T and pET–15b contained two additional GlySer residues or four GlySerHisMet residues, respectively, at their N-termini which are not part of the cortexillin I sequence.

The homogeneity of the recombinant cortexillin I fragments was tested by SDS–PAGE or tricine-SDS–PAGE according to Schägger and von Jagow (1987). Concentrations of the purified proteins were determined by the BCA protein assay (Pierce). If not stated otherwise, all protein samples were dialyzed against 5 mM sodium phosphate buffer (pH 7.4), supplemented with 150 mM NaCl and stored at either 4°C or –70°C for further analysis.

Peptide

The 16 residue peptide cI-t (Ac-ARMELEARLAKTEKDR-NH_2) was purchased from MedProbe (Norway). Purity of the peptide, which was >95%, had been checked by qualitative amino acid and mass spectral analysis. Exact concentrations of peptide solutions were determined by quantitative amino acid analysis.

Analytical ultracentrifugation (AUC)

AUC was performed according to Faix *et al.* (1996). Unless stated otherwise, the recombinant cortexillin I rod fragments were analyzed at 20°C in 5 mM sodium phosphate buffer (pH 7.4) supplemented with 150 mM NaCl, and protein concentrations were adjusted to 0.1–0.5 mg/ml. Sedimentation equilibrium runs were performed on a Beckman Optima XL-A analytical centrifuge equipped with an An-60ti rotor at 24 000 r.p.m. for Ir, Ir-2hC, Ir-3hC, Ir-4hC and Ir-6hN, 16 000 r.p.m., 20 000 r.p.m. and 28 000 r.p.m. for Ir-5hC, 34 000 r.p.m. for Ir-6hC, 48 000 r.p.m. for Ir-12hC and Ir-12hN, 16 000 r.p.m. for cI-310, and 21 000 r.p.m. for cI-324. Sedimentation equilibrium runs with the 16 residue peptide cI-t were performed at 56 000, 48 000 and 40 000 r.p.m. For all samples a partial specific volume of 0.73 ml/g was assumed.

Electron microscopy (EM)

Sample preparation for EM was performed as described by Engel (1994). The glycerol-sprayed/rotary metal-shadowed specimens (10–50 μg/ml) were examined in a Philips EM400 TEM operated at 80 kV. Electron micrographs were recorded on Kodak SO-163 electron image film at 40 000 times nominal magnification, which was calibrated according to Wrigley (1968). Molecular length distributions of Ir were measured from micrograph areas enlarged ten times, plotted as histograms and fitted by single Gaussian curves using a Marquaradt curve fitting software (Sigma Plot, Jandel Scientific).

Circular dichroism (CD) spectroscopy

Far-UV CD spectra and thermal unfolding profiles were recorded on a Cary 61 spectropolarimeter equipped with a temperature-controlled quartz cell of 0.1 cm pathlength as described by Kammerer *et al.* (1995). A ramping rate of 1°C/min was used for all experiments. CD analysis of the peptide cI-t was carried out on a Jasco J 720 spectro-polarimeter equipped with a temperature-controlled quartz cell of 0.5 cm pathlength. Spectra represent averages of ten accumulations. Data were evaluated with the Jasco J 720 (Japan Scientific) and Sigma Plot (Jandel Scientific) software.

1-anilino-8-naphthalenesulfonate (ANS) binding studies

Fluorescence studies of binding to ANS were performed as described in Jelesarov and Bosshard (1996) in a Jasco FP-777 spectrofluorimeter by measuring the change in fluorescence emission between 400 and 600 nm (excitation 350 nm).

Acknowledgements

We are especially indebted to Dr J.Engel for fruitful discussion and support. We thank Dr C.-A.Schoenenberger for critical review of the manuscript. We are grateful to Dr M.Gesemann, Mr F.Wohnsland and Mr D.Fotiadis for excellent technical assistance. This work was supported by grants of the Swiss National Science Foundation, by the Canton Basel-Stadt and by the Maurice Müller Foundation of Switzerland.

References

Beck,K., Gambee,J.E., Kamawal,A. and Bächinger,H.P. (1997) A single amino acid can switch the oligomerization state of the α-helical coiled-coil domain of cartilage matrix protein. *EMBO J.*, **16**, 3767–3777.

Betz,S.F., Bryson,J.W. and DeGrado,W.F. (1995) Native-like and structurally characterized designed α-helical bundles. *Curr. Opin. Struct. Biol.*, **5**, 457–463.

Brandenberger,R., Kammerer,R.A., Engel,J. and Chiquet,M. (1996) Native chick laminin-4 containing the β2 chain (s-laminin) promotes motor axon growth. *J. Cell Biol.*, **135**, 1583–1592.

Brown,J.H., Cohen,C. and Parry,D.A.D. (1996) Heptad breaks in α-helical coiled coils: stutters and stammers. *Proteins*, **26**, 134–145.

Chen,Y.-H., Yang,J.T. and Chau,K.H. (1974) Determination of the helix and β form of proteins in aqueous solution by circular dichroism. *Biochemistry*, **13**, 3350–3359.

Cohen,C. and Parry,D.A.D. (1990) α-Helical coiled-coils and bundles: how to design an α-helical protein. *Proteins*, **7**, 1–15.

Conway,J.F. and Parry,D.A.D. (1991) Three-stranded α-fibrious proteins: the heptad repeat and its implications for structure. *Int. J. Biol. Macromol.*, **13**, 14–16.

Crick,F.H.C. (1953) The packing of α-helices: simple coiled-coils. *Acta Crystallogr.*, **6**, 689–697.

Dyson,H.J. and Wright,P.E. (1993) Peptide conformation and protein folding. *Curr. Opin. Struct. Biol.*, **3**, 60–65.

Eaton,W.A., Muñoz,V., Thompson,P.A., Chan,C.-K. and Hofrichter,J. (1997) Submillisecond kinetics of protein folding. *Curr. Opin. Struct. Biol.*, **7**, 10–14.

Engel,J. (1994) Electron microscopy of extracellular matrix components. *Methods Enzymol.*, **245**, 469–488.

Fairman,R., Chao,H.-G., Mueller,L., Lavoie,T.B., Shen,L., Novotny,Y. and Matsueda,G.R. (1995) Characterization of a new four-chain coiled-coil: influence of chain length on stability. *Protein Sci.*, **4**, 1457–1469.

Faix,J. *et al.* (1996) Cortexillins, major determinants of cell shape and size, are actin-bundling proteins with a parallel coiled-coil tail. *Cell*, **86**, 631–642.

Fraser,R.D.B., MacRae,T.P. and Miller,A. (1964) The coiled-coil model of α-keratin structure. *J. Mol. Biol.*, **10**, 147–156.

Gilmanshin,R., Williams,S., Callender,R.H., Woodruff,W.H. and Dyer,R.B. (1997) Fast events in protein folding: relaxation dynamics of secondary and tertiary structure in native apomyoglobin. *Proc. Natl Acad. Sci. USA*, **94**, 3709–3713.

Harbury,P.B., Zhang,T., Kim,P.S. and Alber,T. (1993) A switch between two-, three-, and four-stranded coiled-coils in GCN4 leucine zipper mutants. *Science*, **262**, 1401–1407.

Harbury,P.B., Kim,P.S. and Alber,T. (1994) Crystal structure of an isoleucine-zipper trimer. *Nature*, **371**, 80–83.

Hodges,R.S. (1996) *De novo* design of α-helical proteins: basic research to medical applications. *Biochem. Cell Biol.*, **74**, 133–154.

Jelesarov,I. and Bosshard,H.R. (1996) Thermodynamic characterization of the coupled folding and association of heterodimeric coiled coils (leucine zippers). *J. Mol. Biol.*, **263**, 344–358.

Kammerer,R.A. (1997) α-Helical coiled-coil oligomerization domains in extracellular proteins. *Matrix Biol.*, **15**, 555–565.

Kammerer,R.A., Antonsson,P., Schulthess,T., Fauser,C. and Engel,J. (1995) Selective chain recognition in the C-terminal α-helical coiled-coil region of laminin. *J. Mol. Biol.*, **250**, 64–73.

Kammerer,R.A., Schulthess,T., Landwehr,R., Lustig,A. and Engel,J. (1998) Tenascin-C hexabrachion assembly is a sequential two-step process initiated by coiled-coil α-helices. *J. Biol. Chem.*, in press.

King,L., Seidel,J.C. and Lehrer,S.S. (1995) Unfolding domains in smooth muscle myosin rod. *Biochemistry*, **34**, 6770–6774.

Kohn,W.D., Mant,C.T. and Hodges,R.S. (1997) α-Helical protein assembly motifs. *J. Biol. Chem.*, **272**, 2583–2586.

Lehrer,S.S. (1978) Effects of an interchain disulfide bond on tropomyosin structure: intrinsic fluorescence and circular dichroism studies. *J. Mol. Biol.*, **118**, 209–226.

Lumb,K.J., Carr,C.M. and Kim,P.S. (1994) Subdomain folding of the coiled coil leucine zipper from the bZIP transcriptional activator GCN4. *Biochemistry*, **33**, 7361–7367.

Lupas,A. (1996) Coiled coils: new structures and new functions. *Trends Biochem. Sci.*, **21**, 375–382.

Lupas,A., Van Dyke,M. and Stock,J. (1991) Predicting coiled coils from protein sequences. *Science*, **252**, 1162–1164.

Malashkevich,V.N., Kammerer,R.A., Efimov,V.P., Schulthess,T. and Engel,J. (1996) The crystal structure of a five-stranded coiled coil in COMP: a prototype ion channel? *Science*, **274**, 761–765.

Marqusee,S. and Baldwin,R.L. (1987) Helix stabilization by $Glu^{-}...Lys^{+}$ salt bridges in short peptides of *de novo* design. *Proc. Natl Acad. Sci. USA*, **84**, 8898–8902.

Matsudaira,P. (1991) Modular organization of actin crosslinking proteins. *Trends Biochem. Sci.*, **16**, 87–92.

McLachlan,A.D. and Stewart,M. (1975) Tropomyosin coiled-coil interactions: evidence for an unstaggered structure. *J. Mol. Biol.*, **98**, 293–304.

Mo,J., Holtzer,M.E. and Holtzer,A. (1991) Kinetics of self-assembly of αα-tropomyosin coiled coils from unfolded chains. *Proc. Natl Acad. Sci. USA*, **88**, 916–920.

Mo,J., Holtzer,M.E. and Holtzer,A. (1992) Kinetics of folding and unfolding of ββ-tropomyosin. *Biopolymers*, **32**, 1581–1587.

Monera,O.D., Kay,C.M. and Hodges,R.S. (1994) Electrostatic interactions control the parallel and antiparallel orientation of α-helical chains in double-stranded α-helical coiled-coils. *Biochemistry*, **33**, 3862–3871.

O'Shea,E.K., Rutkowski,R., Stafford III,W.F. and Kim,P.S. (1989) Preferential heterodimer formation by isolated leucine zippers from Fos and Jun. *Science*, **245**, 646–648.

O'Shea,E.K., Klemm,J.D., Kim,P.S. and Alber,T. (1991) X-ray structure of the GCN4 leucine zipper, a two-stranded, parallel coiled coil. *Science*, **254**, 539–544.

O'Shea,E.K., Rutkowski,R. and Kim,P.S. (1992) Mechanism of specificity in the Fos–Jun oncoprotein heterodimer. *Cell*, **68**, 699–708.

Parthasarathy,R., Chaturvedi,S. and Go,K. (1995) Design of α-helical peptides: their role in protein folding and molecular biology. *Prog. Biophys. Mol. Biol.*, **64**, 1–54.

Schägger,H. and von Jagow,G. (1987) Tricine-sodium dodecyl sulfate–polyacrylamide gel electrophoresis for the separation of proteins in the range from 1 to 100 kDa. *Anal. Biochem.*, **166**, 368–379.

Shoemaker,K.R., Fairman,R., Kim,P.S., York,E.J., Stewart,J.M. and Baldwin,R.L. (1987) The C-peptide helix from ribonuclease A considered as an autonomous folding unit. *Cold Spring Harbor Symp. Quant. Biol.*, **52**, 391–398.

Scholtz,J.M. and Baldwin,R.L. (1992) The mechanism of α-helix formation by peptides. *Annu. Rev. Biophys. Biomol. Struct.*, **21**, 95–118.

Sodek,J., Hodges,R.S., Smillie,L.B. and Jurasek,L. (1972) Amino-acid sequence of rabbit skeletal tropomyosin and its coiled-coil structure. *Proc. Natl Acad. Sci. USA*, **69**, 3800–3804.

Sosnick,T.R., Jackson,S., Wilk,R.R., Englander,S.W. and DeGrado,W.F. (1996) The role of helix formation in the folding of a fully α-helical coiled coil. *Proteins*, **24**, 427–432.

Stryer,L. (1965) The interaction of naphtalene dye with apomyoglobin and apohemoglobin. A fluorescent probe of non-polar binding sites. *J. Mol. Biol.*, **13**, 482–495.

Su,J.Y., Hodges,R.S. and Kay,C.M. (1994) Effect of chain length on the formation and stability of synthetic α-helical coiled coils. *Biochemistry*, **33**, 15501–15510.

Thompson,K.S., Vinson,C.R. and Freire,E. (1993) Thermodynamic characterization of the structural stability of the coiled-coil region of the bZIP transcription factor GCN4. *Biochemistry*, **32**, 5491–5496.

Tripet,B., Vale,R.D. and Hodges,R.S. (1997) Demonstration of coiled-coil interactions within the kinesin neck region using synthetic peptides. *J. Biol. Chem.*, **272**, 8946–8956.

Trybus,K.M., Freyzon,Y., Faust,L.Z. and Sweeney,H.L. (1997) Spare the rod, spoil the regulation: necessity for myosin rod. *Proc. Natl Acad. Sci. USA*, **94**, 48–52.

Wendt,H., Berger,C., Baici,A., Thomas,R.M. and Bosshard,H.R. (1995) Kinetics of folding of leucine zipper domains. *Biochemistry*, **34**, 4097–4107.

Wendt,H., Leder,L., Härmä,H., Jelesarov,I., Baici,A. and Bosshard,H.R. (1997) Very rapid, ionic strength-dependent association and folding of a heterodimeric leucine zipper. *Biochemistry*, **36**, 204–213.

Williams,S., Causgrove,T.B., Gilmanshin,R., Fang,K.S., Callender,R.H.,Woodruff, W.H. and Dyer,R.B. (1996) Fast events in protein folding: helix melting and formation in a small peptide. *Biochemistry*, **35**, 691–697.

Wrigley,N.G. (1968) The lattice spacing of crystalline catalase as an internal standard of length in electron microscopy. *J. Ultrastruct. Res.*, **24**, 454–464.

Zhou,N.E., Kay,C.M. and Hodges,R.S. (1992) Synthetic model proteins: the relative contribution of leucine residues at the nonequivalent positions of the 3–4 hydrophobic repeat to the stability of the two-stranded α-helical coiled-coil. *Biochemistry*, **31**, 5739–5746.

Zhou,N.E., Kay,C.M. and Hodges,R.S. (1994) The role of interhelical ionic interactions in controlling protein folding and stability. *J. Mol. Biol.*, **237**, 500–512.

Zitzewitz,J.A., Bilsel,O., Luo,J., Jones,B.E. and Matthews,C.R. (1995) Probing the folding mechanism of a leucine zipper peptide by stopped-flow circular dichroism spectroscopy. *Biochemistry*, **34**, 12812–12819.

Received December 4, 1997; revised January 15, 1998; accepted February 10, 1998